Nardostachin from *Nardostachys jatamansi* exerts anti-neuroinflammatory effects through TLR4/MyD88-related suppression of the NF-κB and JNK MAPK signaling pathways in lipopolysaccharide-induced BV2 and primary microglial cells

DONG-CHEOL KIM[1,2*], JIN-SOO PARK[1*], CHI-SU YOON[3], YOUN-CHUL KIM[1,2] and HYUNCHEOL OH[1,2]

[1]College of Pharmacy and [2]Hanbang Cardio-Renal Syndrome Research Center, Wonkwang University, Iksan, Jeollabuk-do 54538; [3]Korea Research Institute of Bioscience and Biotechnology, Yeongudanji-ro, Cheongwon 28116, Republic of Korea

Received January 27, 2020; Accepted October 16, 2020

DOI: 10.3892/mmr.2020.11720

Abstract. Through searching for anti-neuroinflammatory metabolites from *Nardostachys jatamansi* extracts, nardostachin was revealed to exert anti-neuroinflammatory effects against lipopolysaccharide (LPS)-induced overproduction of nitric oxide and prostaglandin E2 in BV2 and rat primary microglial cells. Furthermore, nardostachin inhibited the production of inducible nitric oxide synthase and cyclooxygenase-2 as well as pro-inflammatory cytokines, including interleukin (IL)-1β, IL-6, IL-12 and tumor necrosis factor-α in LPS-stimulated BV2 and rat primary microglial cells. In a mechanistic study, nardostachin exhibited inhibitory activity on the nuclear factor (NF)-κB signaling pathway in LPS-stimulated BV2 and rat primary microglial cells by repressing IκB-α phosphorylation and blocking NF-κB translocation. Furthermore, nardostachin exhibited inhibitory effects on LPS-induced phosphorylation of c-Jun N-terminal kinase (JNK) mitogen-activated protein kinase (MAPK). Additionally, nardostachin repressed protein expression of Toll-like receptor 4 (TLR4) and myeloid differentiation factor 88 (MyD88) in LPS-induced BV2 and rat primary microglial cells. These results suggested that nardostachin exerts anti-neuroinflammatory effects on LPS-induced BV2 and rat primary microglial cells by suppressing the TLR4-MyD88-NF-κB and JNK MAPK pathways.

Correspondence to: Professor Youn-Chul Kim or Professor Hyuncheol Oh, College of Pharmacy, Wonkwang University, 460 Iksandae-ro, Iksan, Jeollabuk-do 54538, Republic of Korea
E-mail: yckim@wku.ac.kr
E-mail: hoh@wku.ac.kr

*Contributed equally

Key words: anti-neuroinflammation, nardostachin, *Nardostachys jatamansi*, mitogen-activated protein kinase, nuclear factor-κB

Introduction

Microglia cells are resident macrophages of the central nervous system (CNS) that are essential components of the innate immune response to external pathogen infections, cell debris and CNS injuries (1,2). In response to stimuli, microglia express extensive pattern recognition receptors belonging to the Toll-like receptor (TLR) family and rapidly release various pro-inflammatory and neurotoxic mediators, including reactive oxygen species (ROS), prostaglandin E_2 (PGE_2), nitric oxide (NO) and cytokines, including interleukin (IL)-6, IL-12, tumor necrosis factor-α (TNF-α) and IL-1β. Excessive stimulation leads to neuronal death, resulting in neurodegenerative diseases (3), including Alzheimer's disease (AD), Parkinson's disease (PD), cerebral ischemia, multiple sclerosis and stroke (4-6).

Lipopolysaccharides (LPSs) have been demonstrated to induce the activation of microglial cell pathways (7). Activation of Toll-like receptor 4 (TLR4) is preceded by the binding of LPS, which regulates microglial activation of various signal transduction pathways involved in inflammatory reactions (8). Stimulated TLR4 delivers signals via two major downstream pathways: i) the Toll/IL-1 receptor domain-containing adapter-mediated induction of the interferon-β (TRIF)-dependent pathway (9); and ii) the TLR4-mediated myeloid differentiation factor 88 (MyD88)-dependent pathway. MyD88 regulates the signaling pathway for the majority of TLRs that mediate the activation of nuclear factor-κB (NF-κB) and mitogen-activated protein kinases (MAPKs) (10).

NF-κB serves a critical role in the regulation of inflammatory and immune reactions. When inactive, NF-κB is resident as a cytoplasmic p50/p65 dimer complexed with the NF-κB inhibitor κB (IκB), forming the NF-κB-IκB complex. By contrast, activation of NF-κB by LPS leads to proteasomal degradation and phosphorylation of IκB, allowing the p50/p65 dimer to translocate to the nucleus. The translocated p50/p65 dimer binds to κB, a DNA-binding site, leading to transcription of various genes, including those encoding ROS, PGE_2, NO, IL-6, IL-12, TNF-α and IL-1β (11).

Among the intracellular signaling pathways associated with pro-inflammatory mediator production, MAPK cascades appear to perform vital functions (12,13). Cellular processes, including stress response, differentiation, apoptosis and immune defense, are associated with MAPKs. MAPK has three major subfamilies that are associated with modulation of the inflammatory process: extracellular signal-regulated kinase (ERK), c-Jun N-terminal kinase (JNK) and p38. Previous studies have reported natural products with anti-neuroinflammatory effects that function via inhibiting the NF-κB and MAPK signaling pathways (14,15).

In Tibet, India and China, *Nardostachys jatamansi* DC (Valerianaceae) is a vital traditional medicinal plant used to treat mental disorders, hypertension, convulsions and hyperlipidemia (16). In a recent study, *N. jatamansi* extracts were reported to decrease beta amyloid-activated toxicity in SH-SY5Y cells (17). Its aqueous extracts appeared to protect against cardiac hypertrophy in a 2K1C-induced rat model (18). Furthermore, various sesquiterpenoids isolated from *N. jatamansi* have been demonstrated to mediate the serotonin transport system (19). *N. jatamansi* contains various potentially bioactive chemical components, including monoterpenoids, sesquiterpenoids, triterpenoids and lignans. Recently, sesquiterpenoids from *N. jatamansi* were demonstrated to inhibit the increase in the levels of pro-inflammatory cytokines, including IL-1β, IL-12 and TNF-α, as well as of pro-inflammatory mediators, including NO and PGE_2, in LPS-stimulated BV2 microglial cells (20,21).

Materials and methods

Instruments and isolation of nardostachin. Nuclear magnetic resonance (NMR) spectra were obtained in CDCl3 using a JEOL JNM ECP-400 spectrometer. Chemical shifts were referenced relative to the residual solvent peak (δH/δC = 7.26/77.2). Electrospray ionization mass spectrometry (ESI-MS) data were obtained using an ESI quadrupole time-of-flight MS/MS system (AB SCIEX Pte. Ltd.). High-performance liquid chromatography (HPLC) separation was performed using a YOUNGLIN-YL9100 system (Young Lin Instrument Co., Ltd.) and a Phenomenex Synergi 4 μm Polar-RP 80A, AXIA packed column (21.2x150 mm, 5 μm particle size, 2 mg of the sample injection, 25˚C) with a flow rate of 5 ml/min. All solvents used for HPLC were of analytical grade.

N. jatamansi hexane fraction (GSH-H) was subjected to Si column chromatography (75x330 mm) and eluted with $CHCl_3$-MeOH (70:1-1:1), which yielded seven sub-fractions (GSH-H1-7). Sub-fraction GSH-H3 was subjected to Si column chromatography (70x300 mm) and eluted with hexane-EtOAc (20:1-1:1), which yielded six sub-fractions (GSH-H3-1-6). Sub-fraction GSH-H3-5 was subjected to Si column chromatography (70x280 mm) and eluted with hexane-EtOAc (10:1-1:1), which yielded 12 sub-fractions (GSH-H3-5-1-12). Sub-fraction GSH-H3-5-9 (370.7 mg) was subjected to Si column chromatography (180x30 mm) and eluted with MeOH-$CHCl_3$ (30:1-1:1), which yielded nine sub-fractions (GSH-H3-5-9-1-9). Sub-fraction GSH-H3-5-9-2 (22.0 mg) was further purified using semi-preparative reversed-phase HPLC (20x150 mm), eluting in a gradient of 35-100% ACN in H_2O for over 50 min, which yielded GSH-H3-5-9-2-2 (4.0 mg, tR = 30.9 min).

Nardostachin: Pale yellow powder; ^{1}H-NMR (400 MHz, $CDCl_3$,): δ 6.30 (1H, brs, H-3), 5.94 (1H, d, *J* = 4.2, H-1), 4.57 (1H, d, *J* = 12.2, H-11), 4.37 (1H, d, *J* = 12.2, H-11), 4.17 (1H, m, H-7), 2.92 (1H, q, H-5), 1.12 (3H, d, *J* = 6.8, H-10), 0.97 (3H, d, *J* = 6.59, H-4'), 0.97 (3H, d, *J* = 6.59, H-5'), 0.97 (3H, d, *J* = 6.59, H-4''), 0.97 (3H, d, *J* = 6.59, H-5''); ^{13}C-NMR (100 MHz, $CDCl_3$) δ: 172.1 (C-1''), 172.1 (C-1'), 139.6 (C-3), 114.3 (C-4), 91.6 (C-1),74.7 (C-7), 63.8 (C-11), 44.9 (C-9), 43.6 (C-2'), 43.6 (C-2''), 40.6 (C-8), 39.8 (C-6), 32.1 (C-5), 25.9 (C-3'), 25.8 (C-3''), 22.5 (C-4'), 22.5 (C-5'), 22.5 (C-4''), 22.5(C-5''), 12.8 (C-10); HRESIMS *m/z* 391.2092 [M + Na^+] (calculated for $C_{20}H_{32}O_6Na$ 391.2097).

Chemicals and reagents. Tissue culture reagents, including RPMI-1640 medium and fetal bovine serum (FBS), were purchased from Gibco; Thermo Fisher Scientific, Inc. All other chemicals were obtained from Sigma-Aldrich; Merck KGaA. Primary antibodies against IκB-α (cat. no. 4812, 1:1,000, rabbit), p-IκB-α (cat. no. 2859, 1:1,000, rabbit), p65 (cat. no. 8242, 1:1,000, rabbit), TLR4 (cat. no. 14358, 1:1,000, rabbit), MyD88 (cat. no. 4283, 1:1,000, rabbit), p-ERK (cat. no. 9101, 1:1,000, rabbit), ERK (cat. no. 9102, 1:1,000, rabbit), p-JNK (cat. no. 9251, 1:1,000, rabbit), JNK (cat. no. 9252, 1:1,000, rabbit), p-p38 (cat. no. 9211, 1:1,000, rabbit) and p38 (cat. no. 9212, 1:1,000, rabbit) were obtained from Cell Signaling Technology, Inc. Antibody against inducible nitric oxide synthase (iNOS; cat. no. 160862, 1:1,000, rabbit) was obtained from Cayman Chemical and against cyclo-oxygenase-2 (COX-2; cat. no. ab15191, 1:1,000, rabbit) from Abcam. Antibodies against p50 (cat. no. sc-7178; 1:1,000, rabbit), β-actin (cat. no. sc-47778; 1:1,000, rabbit) and PCNA (cat. no. sc-56, 1:1,000, mouse) were purchased from Santa Cruz Biotechnology. Anti-mouse, anti-goat, and anti-rabbit secondary antibodies were purchased from Merck Millipore ELISA kits for PGE_2 were purchased from R&D Systems, Inc (cat. no. KGE004B).

Cell culture and viability assay. BV2 microglial cells were maintained at a density of $5x10^5$ cells/ml in RPMI-1640 medium, supplemented with 10% heat-inactivated FBS, penicillin G (100 U/ml), streptomycin (100 mg/ml) and L-glutamine (2 mM), and were incubated at 37˚C in a humidified atmosphere containing 5% CO_2. Primary microglial cells were cultured from the cerebral cortices or substantia nigra of 1-day-old Sprague-Dawley rats weighing 6-8 g which were purchased from the Orient Co., Ltd. Rats were housed in standard cages in a climate-controlled room with an ambient temperature of 23±2˚C only for 3 h and then were sacrificed. A total of 15 rats were used in the isolation of primary microglial cells. Brain tissues were triturated into single cells in Dulbecco's modified Eagle's medium containing 10% FBS and cultured in 75-cm^2 T-flasks for 2 weeks in a humified incubator at 37˚C. The microglial cells were detached from the flasks by mild shaking and applied to a strainer to remove astrocytes and cell clumps. Cells were plated onto 6-well plates ($5x10^5$ cells/ml) with B27® supplement (Thermo Fisher Scientific, Inc.) in the absence of insulin for 2-3 days. Cells were washed to remove unattached cells prior to use in subsequent experiments.

Cell viability was evaluated by determining mitochondrial reductase function using an assay based on reducing MTT into formazan crystals. The formation of formazan is proportional to the number of functional mitochondria in living cells. Cells were maintained at $1x10^5$ cells/ml in each well of the 96-well plate to determine cell viability. Following incubation for 6 h, the cells were treated for 24 h with the indicated concentrations of 1.0. 4.0 μM nardostachin with or without LPS (1 μg/ml). Next, 50 μl MTT (2.5 mg/ml) was added to each well in fresh medium at a final concentration of 0.5 mg/ml, and the mixture was further incubated for 3-4 h at 37˚C, following which the liquid was removed from the wells. Next, the formazan formed was dissolved in 150 μl dimethyl sulfoxide, and the optical density was measured at 590 nm wavelength. The optical density of the formazan formed in control (untreated) cells was considered to indicate 100% viability.

Reverse transcription-quantitative polymerase chain reaction (RT-qPCR). Total RNA was isolated from the cells using TRIzol® reagent (Invitrogen; Thermo Fisher Scientific, Inc.), according to the manufacturer's protocols, and quantified spectrophotometrically (at 260 nm wavelength). Total RNA (1 μg) was reverse transcribed using the High Capacity RNA-to-cDNA kit for 65 min at 100˚C (Applied Thermo Fisher Scientific, Inc.). The cDNA was then amplified using the SYBR Premix Ex Taq kit (Takara Bio, Inc.) on a StepOnePlus Real-Time PCR system (Applied Biosystems; Thermo Fisher Scientific, Inc.). In brief, each 20 ml reaction volume contained 10 ml SYBR Green PCR Master Mix, 0.8 mM each primer and diethylpyrocarbonate-treated water. Primer sequences were designed using PrimerQuest (Integrated DNA Technologies, Inc.) and were as follows: TNF-α forward, 5'-CCAGACCCTCACACTCACAA-3' and reverse, 5'-ACAAGGTACAACCCATCGGC-3'; IL-1β forward, 5'-AATTGGTCATAGCCCGCACT-3' and reverse, 5'-AAGCAATGTGCTGGTGCTTC-3'; IL-6 forward, 5'-ACT TCCAAGTCGGAGGCTT-3' and reverse, 5'-TGCAAGTGC ATCATCGTTGT-3'; and IL-12 forward, 5'-AGT GACATG TGGAATGGCGT-3' and reverse, 5'-CAGTTCAATGGG CAGGGTCT-3'. The optimal conditions for PCR amplification of the cDNA were established according to the manufacturer's protocols. The data were analyzed using StepOne software (Applied Biosystems; Thermo Fisher Scientific, Inc.), and the cycle numbers at the linear amplification threshold (Ct) for the endogenous control gene (GAPDH) and target gene were recorded. Relative gene expression (target gene expression normalized to endogenous control gene expression) was calculated using the comparative Ct method ($2^{-\Delta\Delta Ct}$) (22). The analysis was conducted independently three times.

DNA-binding activity of NF-κB. The DNA-binding activity of NF-κB in nuclear extracts was measured using the TransAM kit (cat. no. 40096; Active Motif, Inc.), according to the manufacturer's protocols. BV2 and rat primary microglial cells were pre-treated for 3 h with the indicated concentrations of nardostachin and stimulated for 30 min with LPS (1 μg/ml) at 37˚C, and the nuclear fractions were extracted. The nuclear extracts were added to the oligonucleotide-coated plate and reacted with primary and secondary antibodies each for 1 h at room temperature provided in the kit. A developing buffer was then added to each well, and this buffer reacted with the horseradish peroxidase-conjugated secondary antibodies provided in the kit, yielding a blue color. Next, the stop solution was added, and the optical density was measured at 450 nm wavelength. The assay was conducted independently three times.

Preparation of cytosolic and nuclear fractions. The cytosolic and nuclear fractions were extracted using the Caiman Nuclear Extraction kit from Cayman Chemical (cat. no. 10009277) and each fraction was lysed according to the manufacturer's protocols.

Nitrite (NO production) determination. The nitrite concentration, an indicator of NO production, was measured using the Griess reaction of the culture medium. The detailed procedure for this assay is described in our previous study (23).

PGE_2 assay. The level of PGE_2 present in each sample was determined using a commercially available kit (cat. no. KGE004B) from R&D Systems, Inc. Three independent assays were performed according to the manufacturer's protocols.

Western blot analysis. Western blot analysis was performed as previously described (23). In brief, BV2 and primary microglial cells were harvested by centrifugation at 200 x g for 3 min at 4˚C, washed with phosphate-buffered saline, and lysed using radioimmunoprecipitation assay (RIPA) buffer (Thermo Fisher Scientific, Inc.). The protease and phosphatase inhibitor cocktail (Thermo Fisher Scientific, Inc.) was mixed with RIPA buffer at a 3:100 ratio to evaluate phosphorylation.

Protein concentrations were measured using Bradford protein assay (Bio-Rad Laboratories, Inc.) and normalized to ensure equal amounts of protein were loaded. Subsequently, 30 μg protein from each sample was resolved using 7.5 and 12% sodium dodecyl sulfate-polyacrylamide gel electrophoresis. Proteins were electrophoretically transferred onto a Hybond enhanced chemiluminescence (ECL) nitrocellulose membrane. The membrane was blocked with 5% skimmed milk at 4˚C for 1 h and sequentially incubated with the primary antibodies diluted at 1:1,000 at 4˚C for 1.5 h, and horseradish peroxidase-conjugated secondary antibodies diluted at a rate of 1:1,000 at 4˚C for 1 h, followed by ECL detection. The intensity of the protein signals was quantified using ImageJ software (ver. 1.47; National Institutes of Health). The data represent the means of three independent experiments.

NF-κB Localization and Immunofluorescence. BV2 and primary rat microglial cells were cultured on Lab-Tek II chamber slides and treated as described in the figure legends. The cells were treated with 4.0 μM nardostachin for 1 h, fixed in formalin, permeabilized with cold acetone, and then probed with a primary antibody against NF-κB and a fluorescein Isothiocyanate (FITC)-labeled secondary antibody (Alexa Fluor 488; Invitrogen; Thermo Fisher Scientific, Inc.). To visualize the nuclei, the cells were treated with DAPI (1 μg/ml) for 30 min, washed with PBS for 5 min, and treated with 50 μl VectaShield (Vector Laboratories, Inc.). The stained cells

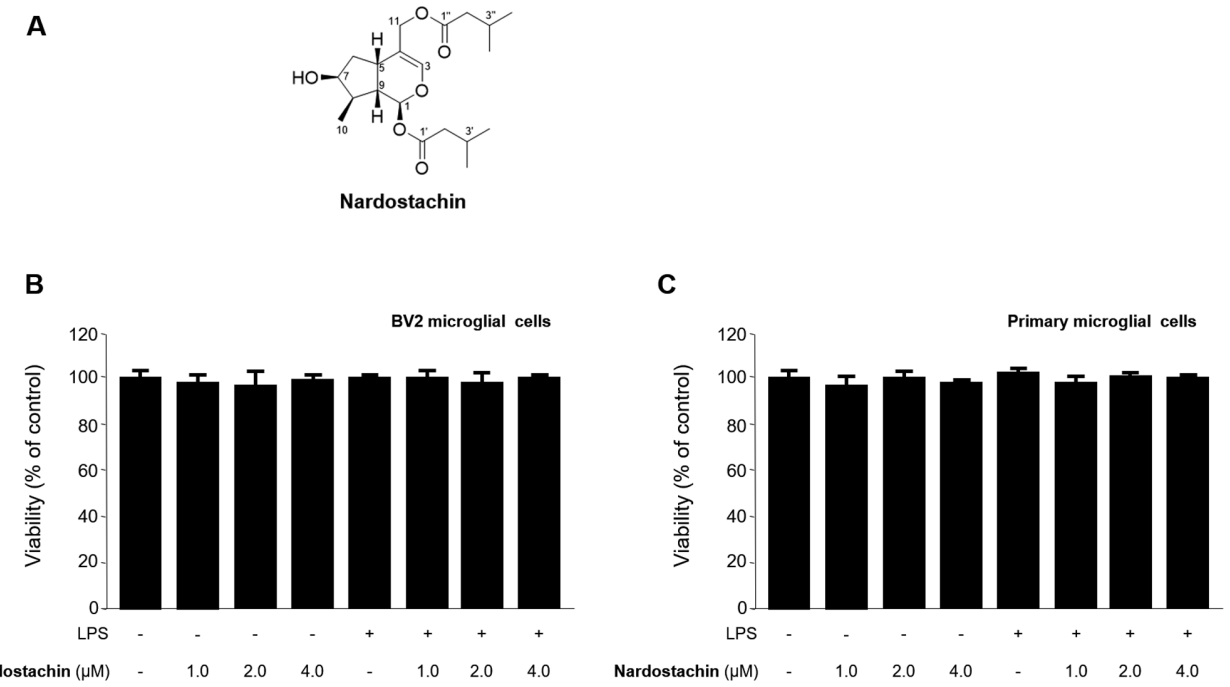

Figure 1. Chemical structure and cytotoxic effects of nardostachin. (A) Chemical structure of the compound was determined by analysis of NMR and MS data. (B and C) Nardostachin induced no cytotoxicity on BV2 and primary microglial cells. BV2 and rat primary microglial cells were incubated for 24 h with various concentrations of nardostachin (1.0-4.0 μM). The bar represents the mean ± standard deviation of three independent experiments.

were visualized and images captured by using a confocal laser microscope (Olympus Corporation).

Statistical analysis. Data are expressed as the mean ± standard deviation of at least three independent experiments. To compare three or more groups, one-way analysis of variance, followed by Tukey's multiple comparison tests, was used. Statistical analysis was performed using GraphPad Prism software, version 3.03 (GraphPad Software, Inc.) (24).

Results

Isolation and structure determination of nardostachin and its effect on BV2 and rat primary microglial cell viability. Nardostachin was isolated from the hexane-soluble fraction of the methanol extracts of *N. jatamansi* using C_{18} flash column chromatography and semi-preparative HPLC (Fig. 1A). The structure of nardostachin was elucidated by analysis of MS and NMR data and a comparison of its spectral data with those reported in the literature (25).

A conventional MTT assay was used to analyze BV2 and rat primary microglial cells treated with different concentrations of nardostachin (1.0-4.0 μM) for 24 h in the absence of LPS to determine the cytotoxicity of nardostachin. As shown in Fig. 1B and C, cell viability was not affected by nardostachin compared with that in the control group. Based on the MTT assay results, the concentration range of nardostachin from 1.0 to 4.0 μM was selected for subsequent experiments.

Effect of nardostachin on NO and PGE_2 production in LPS-stimulated BV2 and rat primary microglial cells. The effects of nardostachin on LPS-induced secretion of NO and PGE_2 was subsequently analyzed using the Griess method and ELISA, respectively, at non-cytotoxic concentrations. As shown in Fig. 2A-D, nardostachin significantly downregulated the excessive secretion of NO and PGE_2 in LPS-stimulated BV2 and rat primary microglial cells at concentrations ranging from 1.0 to 4.0 μM.

Effects of nardostachin on iNOS expression and COX-2 activation in LPS-stimulated BV2 cells and rat primary microglial cells. Since nardostachin was demonstrated to suppress the overproduction of NO and PGE_2 in LPS-induced BV2 and rat primary microglial cells, its effects on iNOS and COX-2 expression in activated BV2 and rat primary microglial cells were investigated. As shown in Fig. 3, LPS (1 μg/ml) induced a 6-7-fold increase in iNOS and COX-2 expression after 24 h of treatment. However, nardostachin treatment (1.0-4.0 μM) attenuated LPS-mediated iNOS and COX-2 expression in a dose-dependent manner.

Effects of nardostachin on pro-inflammatory cytokines in LPS-stimulated BV2 and rat primary microglial cells. Next, the effects of nardostachin on LPS-induced BV2 and rat primary microglial cells were investigated. The mRNA levels of pro-inflammatory cytokines, including TNF-α, IL-6, IL-12 and IL-1β were assayed at non-cytotoxic concentrations. The production of TNF-α, IL-6, IL-12 and IL-1β was increased in the cells treated with LPS alone, whereas the co-treatment of nardostachin with LPS downregulated the overproduction of TNF-α, IL-6, IL-12 and IL-1β mRNA in a dose-dependent manner (Fig. 4).

Effect of nardostachin on NF-κB activation in LPS-stimulated BV2 and rat primary microglial cells. Since stimulation of the NF-κB pathway is a critical step in the inflammatory

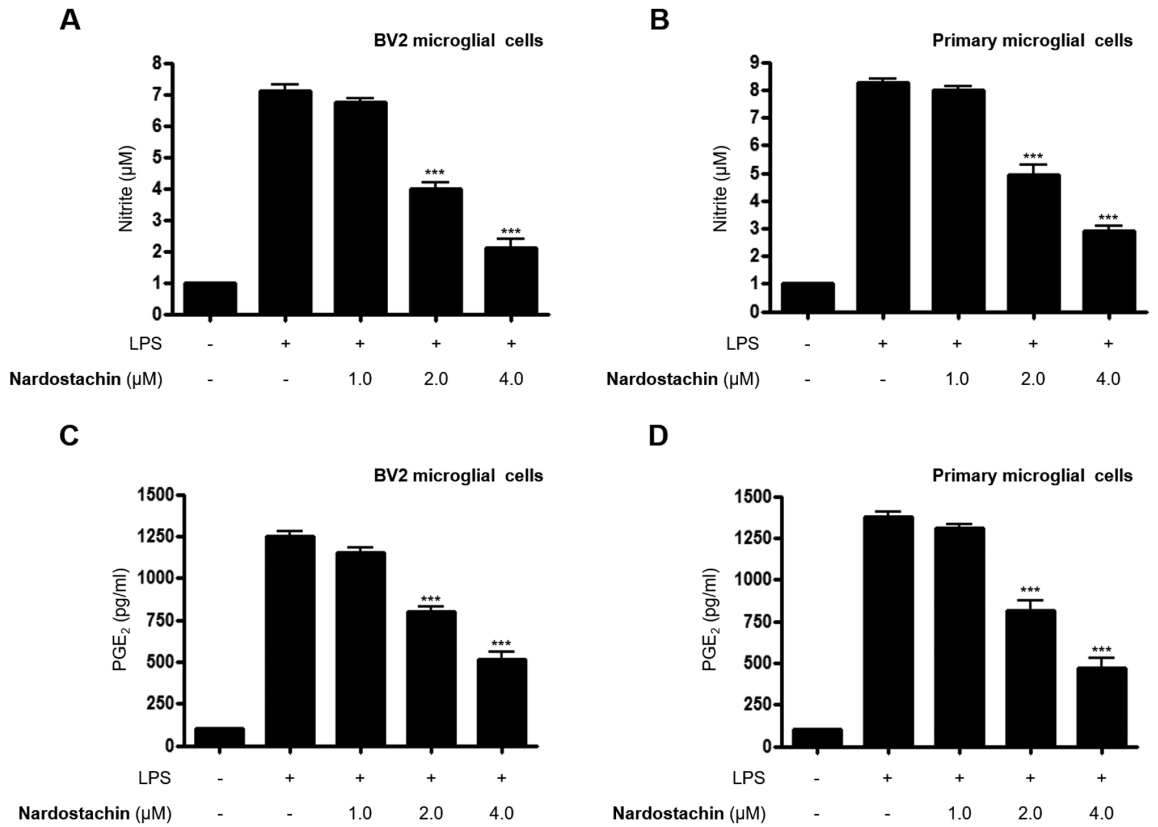

Figure 2. Effects of nardostachin on NO and PGE_2 production in BV2, and rat primary microglial cells stimulated with LPS. (A and C) BV2 cells were pre-treated for 3 h with the indicated concentration of nardostachin, and for 24 h with LPS (1 μg/ml). (B and D) Primary microglial cells were treated under the same conditions. Data represent the mean values of three experiments ± standard deviation. ***P<0.001 vs. the group treated with LPS. NO, nitrous oxide; PGE_2, prostaglandin E_2; LPS, lipopolysaccharide.

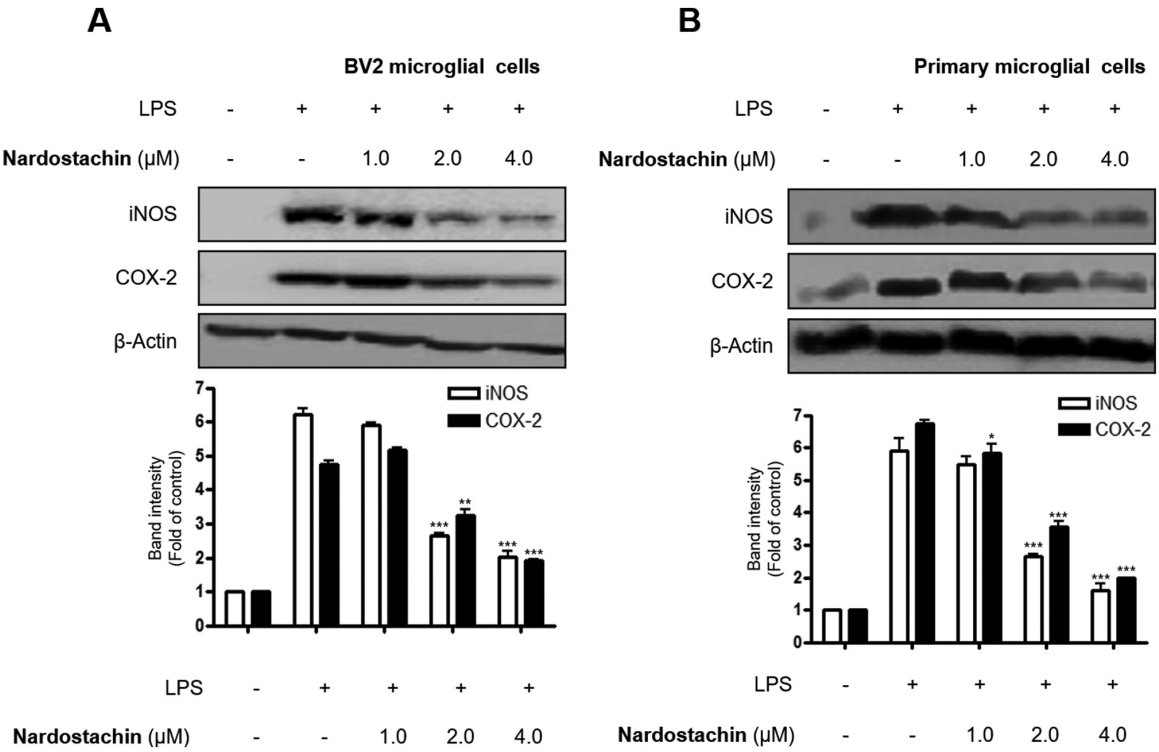

Figure 3. Effects of nardostachin on protein expression of iNOS and COX-2 in BV2 and rat primary microglial cells stimulated with LPS. (A) BV2 cells were pre-treated for 3 h with the indicated concentration of nardostachin, and for 24 h with LPS (1 μg/ml). (B) Primary microglial cells were treated under the same conditions. Western blot analysis was performed and band intensity was quantified by densitometry and normalized to β-actin, the values presented at the bottom of each band. Data represent the mean values of three experiments ± standard deviation. *P<0.05, **P<0.01, ***P<0.001 vs. the group treated with LPS. iNOS, inducible nitric oxide synthase; COX-2, cyclooxygenase 2; LPS, lipopolysaccharide.

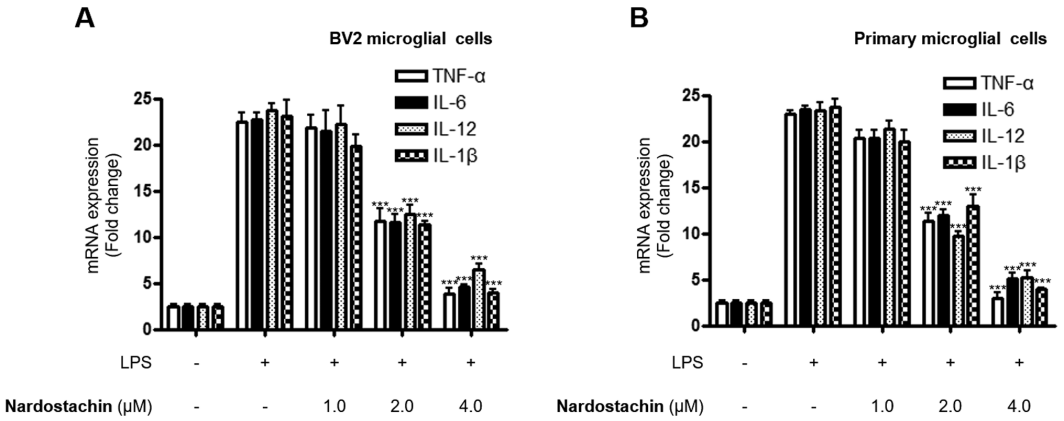

Figure 4. Effects of nardostachin on TNF-α, IL-6, IL-12 and IL-1β mRNA production in BV2 and rat primary microglial cells stimulated with LPS. (A) BV2 cells were pre-treated for 3 h with the indicated concentration of nardostachin, and for 6 h with LPS (1 μg/ml). (B) Primary microglial cells were treated under the same conditions. The mRNA expression of TNF-α, IL-6, IL-12 and IL-1β was determined. Data represent the mean values of three experiments ± standard deviation. ***P<0.001 vs. the group treated with LPS. TNF-α, tumor necrosis factor-α; IL, interleukin; LPS, lipopolysaccharide.

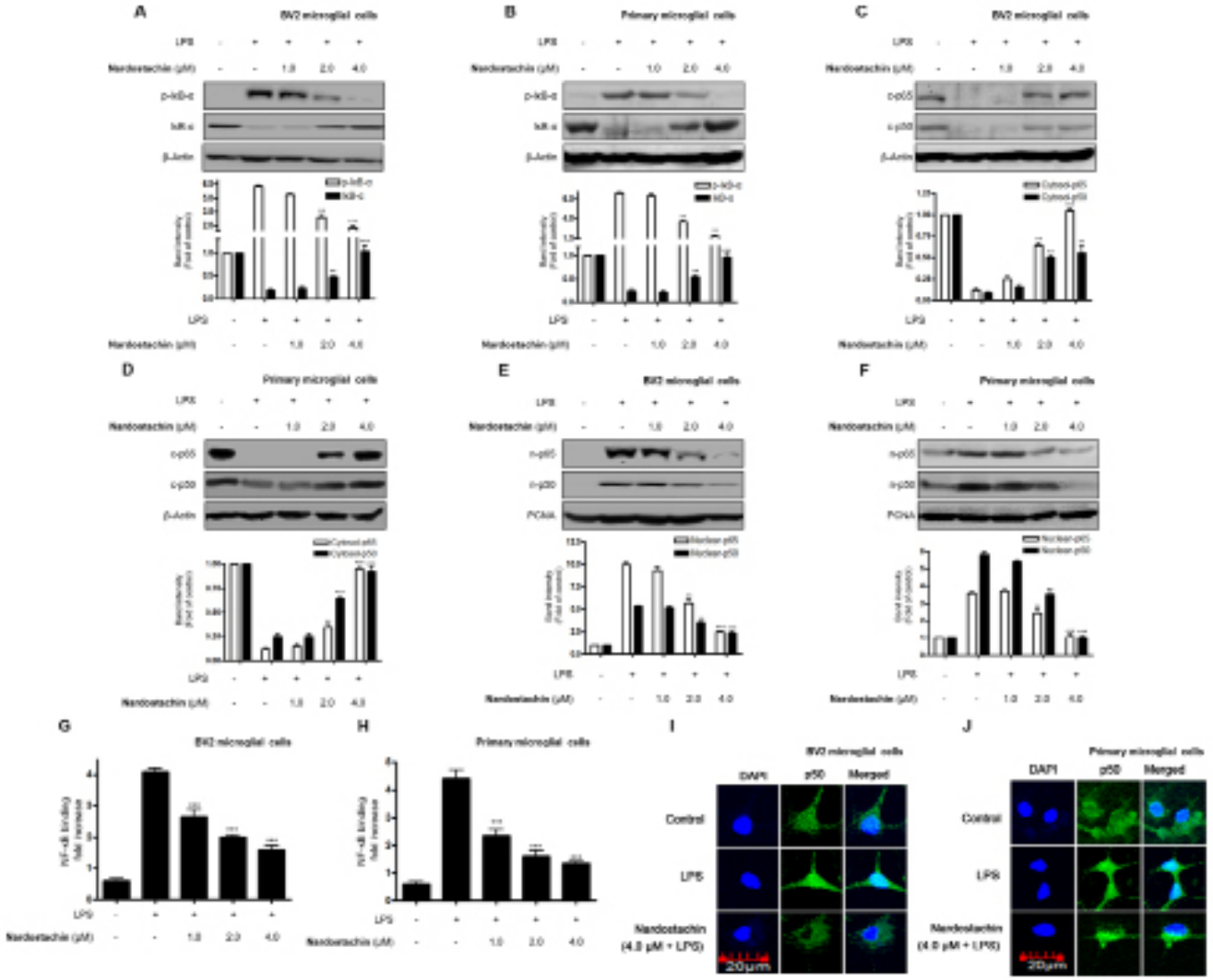

Figure 5. Effect of nardostachin on the activation of the NF-κB pathway in LPS-stimulated BV2 and primary microglial cells. (A-H) Following pretreatment with nardostachin (1.0, 2.0, and 4.0 μM) for 3 h, cells were treated with LPS (1 μg/ml) for 1 h. (A and B) Total proteins were prepared and the western blot analysis was performed using specific IκB-α and p-IκB-α antibodies. (C-F) Cytosol and nuclear extracts were prepared for a western blot of p65 and p50 of NF-κB, using specific anti-p65 and anti-p50 monoclonal antibodies. (G and H) A commercially available NF-κB ELISA (Active Motif) was used to test the nuclear extracts and determine the degree of NF-κB binding. (I and J) Immunofluorescence was performed to evaluate whether nardostachin could inhibit NF-κB translocation from cytosol to nucleus in LPS-stimulated BV2 and primary microglial cells. Band intensity was quantified by densitometry and normalized to β-actin or proliferating cell nuclear antigen (PCNA) band, the values presented at the bottom of each band. Data represent the mean values of three experiments ± standard deviation. **P<0.01, ***P<0.001 vs. the group treated with LPS. NF-κB, nuclear factor κB; LPS, lipopolysaccharide.

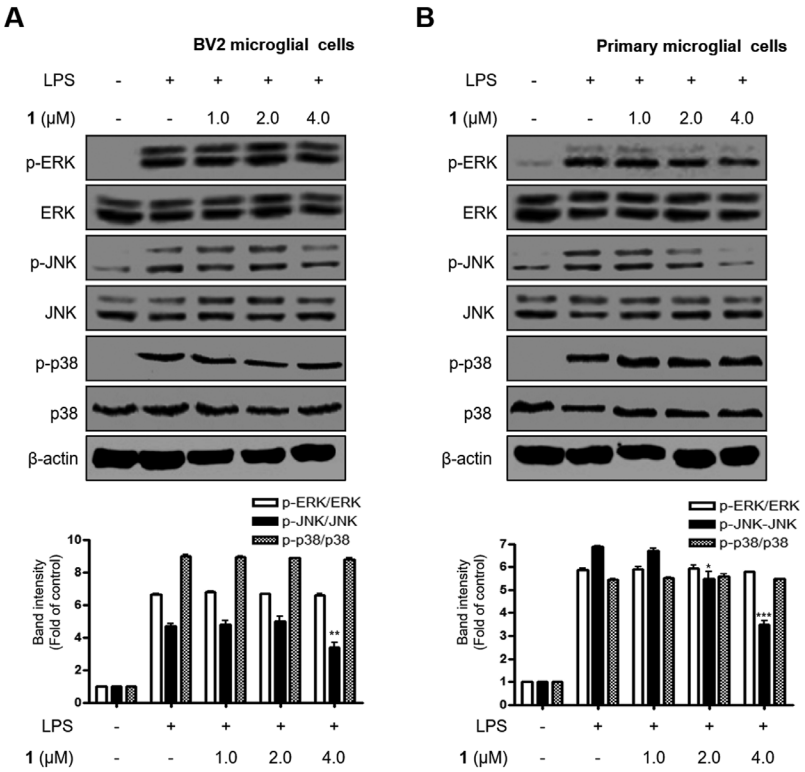

Figure 6. Effects of nardostachin on ERK, JNK and p38 MAPK phosphorylation and protein expression. (A) BV2 cells were pre-treated for 3 h with the indicated concentration of nardostachin, and for 1 h with LPS (1 μg/ml), and (B) primary microglial cells were treated under the same conditions. The levels of p-ERK, p-JNK and p-p38 MAPK were determined by western blot analysis. Representative blots from three independent experiments with similar results and densitometric evaluations are shown. Band intensity was quantified by densitometry and normalized to the total form of each MAPK, the values presented at the bottom of each band. Data represent the mean values of three experiments ± standard deviation. *P<0.05, **P<0.01, ***P<0.001 vs. the group treated with LPS. LPS, lipopolysaccharide; p-ERK, phosphorylated-ERK; p-JNK, phosphorylated-JNK; p-p38 MAPK, phosphorylated-p38 MAPK.

reaction, whether nardostachin inhibits LPS-induced NF-κB activation in LPS-stimulated BV2 and rat primary microglial cells was investigated by examining its effects on NF-κB translocation. As shown in Fig. 5A and B, LPS-stimulated phosphorylation of IκB-α was significantly suppressed by nardostachin. Furthermore, IκB-α was degraded after the cells were stimulated with LPS for 1 h. However, IκBα degradation was markedly inhibited by the pretreatment of the cells with nardostachin. It was also demonstrated to block LPS-stimulated nuclear translocation of the NF-κB p50/p65 dimer. As shown in Fig. 5C-F, the protein expression of cytosolic p65/p50 was decreased, and protein levels of nuclear p65/p50 were increased following stimulation with LPS for 1 h. However, treatment with nardostachin suppressed the LPS-enhanced protein levels of nuclear p65/p50 in a dose-dependent manner. The results of the NF-κB binding assay also indicated that treatment with nardostachin markedly inhibited the DNA-binding activity of NF-κB in the nucleus (Fig. 5G and H). Immunofluorescence analysis indicated the significant translocation of NF-κB/p50 into the nucleus upon LPS stimulation. However, nardostachin pretreatment blocked nuclear translocation in the LPS-induced BV2 and rat primary microglial cells (Fig. 5I and J).

Effects of nardostachin on MAPK phosphorylation in LPS-stimulated BV2 cells and rat primary microglial cells. NF-κB activation is alternatively regulated by the intracellular signaling proteins, MAPKs, in LPS-induced BV2 and rat primary microglial cells (26). Therefore, it was investigated whether nardostachin regulates the phosphorylation of these signaling proteins, which may be activated by LPS in BV2 and rat primary microglial cells. As shown in Fig. 6, LPS-induced phosphorylation of JNK was significantly suppressed by pretreatment of the cells with nardostachin for 3 h. This effect was dose-dependent, suggesting an additional characteristic of nardostachin in regulating LPS-induced inflammation. However, ERK and p38 phosphorylation were unaffected upon exposure to nardostachin (Fig. 6).

Effect of nardostachin on TLR4 expression and its interaction with MyD88 in LPS-induced BV2 and rat primary microglial cells. TLR4 is involved in the regulation of LPS-stimulated inflammatory mediators through stimulation of the NF-κB and MAPK pathways. Therefore, the effect of nardostachin on protein expression of TLR4 was investigated to gain further insight into the mechanism underlying its anti-neuroinflammatory activity. As shown in Fig. 7, TLR4 and MyD88 protein expression was increased in BV2 and rat primary microglial cells upon LPS treatment, whereas pretreatment with nardostachin for 3 h attenuated the LPS-induced TLR4 and MyD88 protein expression in a dose-dependent manner.

Discussion

The activation of microglial cells through TLR-mediated signaling pathways leads to the production of several

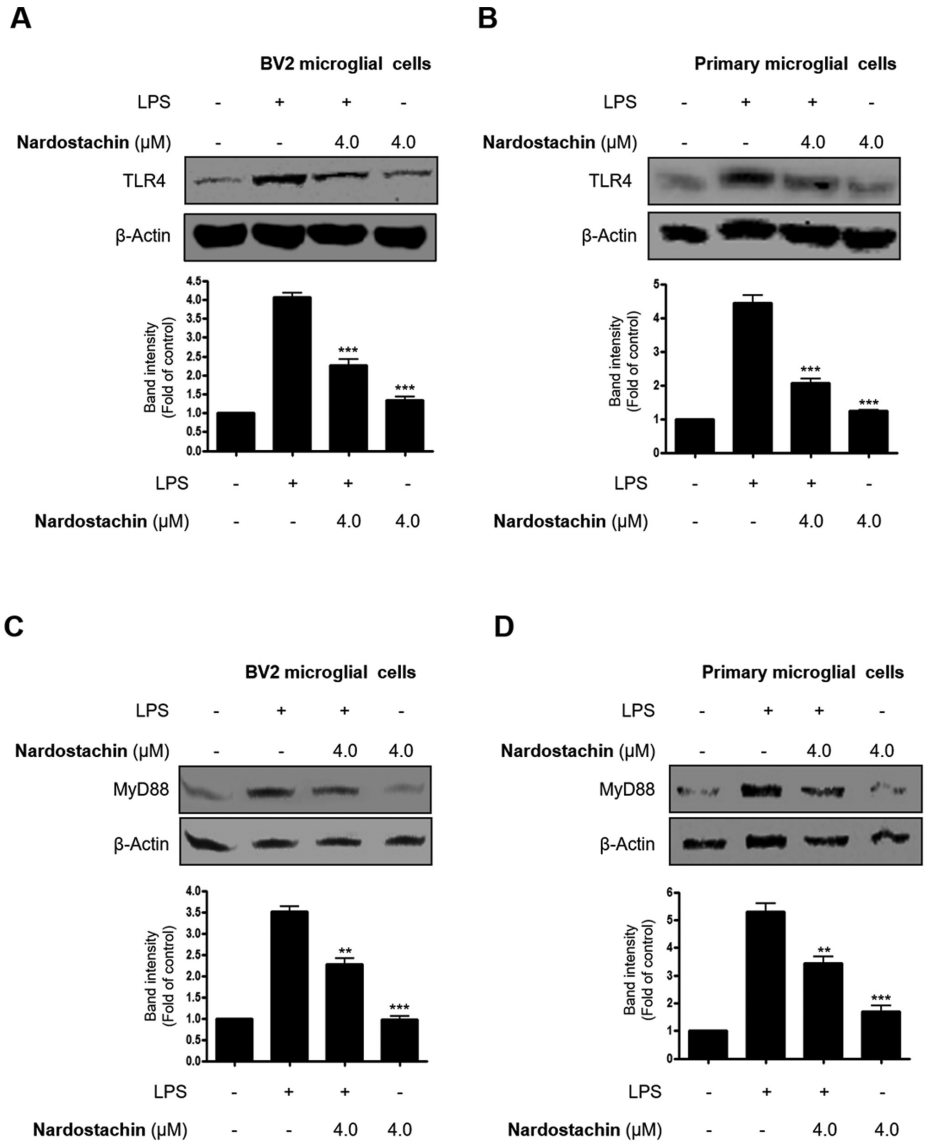

Figure 7. Effects of nardostachin on LPS-induced TLR4 and MyD88 expression in BV2 and rat primary microglial cells. (A and C) BV2 cells were pre-treated for 3 h with the indicated concentration of nardostachin and stimulated for 12 h with LPS (1 μg/ml). (B and D) Primary microglial cells were treated under the same conditions. The protein levels of TLR4 and MyD88 were evaluated by western blot analysis. Band intensity was quantified by densitometry and normalized to β-actin, and the values are presented below each band. Data represent the mean values of three experiments ± standard deviation. **P<0.01, ***P<0.001 vs. the group treated with LPS. LPS, lipopolysaccharide; TLR4, Toll-like receptor 4; MyD88, myeloid differentiation factor 88.

types of inflammatory mediators, and thus to the development of various neurological disorders, including AD, PD, Huntington's disease, multiple sclerosis and amyotrophic lateral sclerosis (27). When the brain is excessively stimulated, microglia release extensive pattern recognition receptors belonging to the TLR family and their MyD88-dependent pathway is activated. MyD88 mediates representative inflammatory pathways like those of NF-κB and MAPK, which leads to the production of various pro-inflammatory cytokines and mediators, including NO and PGE_2, ROS and cytokines, including IL-12, IL-6, TNF-α and IL-1β (28). The present study demonstrated that nardostachin suppressed the TLR4-MyD88-NF-κB and MAPK pathways in LPS-induced BV2 and rat primary microglial cells. iNOS and COX-2 produced inflammatory mediators, including NO and PGE_2 under inflammatory conditions, indicative of inflammation. Nardostachin suppressed the inflammatory reaction via repression of pro-inflammatory mediators, including iNOS-derived NO and COX-2-derived PGE_2 in LPS-induced BV2 and rat primary microglial cells (Fig. 2). LPS stimulated iNOS and COX-2 overproduction in microglial cells, and this overproduction was inhibited by pretreatment with nardostachin (Fig. 3). Furthermore, nardostachin decreased the mRNA overproduction of pro-inflammatory cytokines, including IL-12, IL-6, TNF-α and IL-1β (Fig. 4), which are involved in severe chronic inflammatory disease (29).

NF-κB is triggered by LPS, which activates transcription molecules that regulate the expression of various inflammatory genes. NF-κB heterodimers consist of p65 and p50 that generally exist in combination with IκB-α in the cytoplasm. In response to stimuli, NF-κB is modulated by various proteins, including TRIF, TRAF6, CD14 and TAK1, which have vital roles in phosphorylation and degradation of IκB and translocation to DNA-binding sites (30). Furthermore, translocated

NF-κB binds to the κB site, causing the transcription and translation of various inflammatory genes. Following treatment with nardostachin, LPS-induced IκB-α degradation and NF-κB translocation were decreased in LPS-stimulated BV2 and rat primary microglial cells (Fig. 5A-F). However, nardostachin repressed the NF-κB DNA-binding activity (Fig. 5G and H) and blocked the localization of p50 into the nucleus in LPS-induced BV2 and rat primary microglial cells (Fig. 5G and H).

MAPK intracellular signaling pathways are involved in modulating inflammatory mediators (31). Therefore, whether the anti-inflammatory effects of nardostachin in LPS-challenged microglial cells affected the expression of MAPKs was investigated. The results demonstrated that nardostachin has potent inhibitory effects on JNK MAPK phosphorylation in LPS-stimulated BV2 and rat primary microglial cells (Fig. 6).

TLR family receptors and MyD88 mediate NF-κB and MAPK and regulate the inflammatory reaction in microglial cells. The present study demonstrated that nardostachin suppressed TLR4 and MyD88 protein expression in LPS-stimulated BV2 and rat primary microglial cells (Fig. 7).

There are certain limitations to the present study. The only *in vitro* test performed in the present study was unable to sufficiently elucidate the mechanism of nardostachin. Additionally, experiments using inhibitors associated with the mechanisms identified in the present study were not conducted. For further research, it is necessary to conduct additional experiments using an *in vivo* model and use appropriate inhibitors to explain the detailed mechanisms through which nardostachin exhibits anti-neuroinflammatory effects. In conclusion, the present study demonstrated that nardostachin isolated from *N. jatamansi* showed anti-neuroinflammatory effects through TLR4/MyD88-mediated regulation of the NF-κB and JNK MAPK signaling pathways in LPS-stimulated BV2 and rat-derived primary microglial cells, and these findings suggested that nardostachin has potential for the design and development of a therapeutic agent against neurodegenerative diseases.

Acknowledgements

Not applicable.

Funding

The present study was supported by a Korea Research Foundation of Korea Grant funded by the Korean Government (grant no. NRF-2017R1A5A2015805).

Availability of data and materials

The datasets used and/or analyzed during the current study are available from the corresponding author on reasonable request.

Authors' contributions

DCK performed the experiments associated with the biological evaluation of the compound and wrote the manuscript. JSP and CSY contributed toward the isolation of the compound. YCK organized this study, contributed toward the biological evaluation of the compound, and wrote the manuscript. HO organized this work, contributed toward the compound's isolation and structure determination, and wrote the manuscript. All authors read and approved the final manuscript.

Ethics approval and consent to participate

All experiments were performed according to protocols approved by the Animal Care Committee of Wonkwang University and were approved by the Institution Animal Care and Use Committee (IACUC) Certification of the Wonkwang University, Korea (approval no. WKU18-04)

Patient consent for publication

Not applicable.

Competing interests

The authors declare that they have no competing interests.

References

1. Ransohoff RM and Perry VH: Microglial physiology: Unique stimuli, specialized responses. Annu Rev Immunol 27: 119-145, 2009.
2. Perry VH and Holmes C: Microglial priming in neurodegenerative disease. Nat Rev Neurol 10: 217-224, 2014.
3. Lehnardt S: Innate immunity and neuroinflammation in the CNS: The role of microglia in Toll-like receptor-mediated neuronal injury. Glia 58: 253-263, 2010.
4. Lukiw WJ: Bacteroides fragilis lipopolysaccharide and inflammatory signaling in Alzheimer's disease. Front Microbiol 7: 1544, 2016.
5. Long-Smith CM, Sullivan AM and Nolan YM: The influence of microglia on the pathogenesis of Parkinson's disease. Prog Neurobiol 89: 277-287, 2009.
6. Perry VH, Nicoll JA and Holmes C: Microglia in neurodegenerative disease. Nat Rev Neurol 6: 193-201, 2010.
7. Fan K, Li D, Zhang Y, Han C, Liang J, Hou C, Xiao H, Ikenaka K and Ma J: The induction of neuronal death by up-regulated microglial cathepsin H in LPS-induced neuroinflammation. J Neuroinflammation 12: 54, 2015.
8. Medzhitov R: Toll-like receptors and innate immunity. Nat Rev Immunol 1: 135-145, 2001.
9. Noman AS, Koide N, Khuda II, Dagvadorj J, Tumurkhuu G, Naiki Y, Komatsu T, Yoshida T and Yokochi T: Thalidomide inhibits lipopolysaccharide-induced nitric oxide production and prevents lipopolysaccharide-mediated lethality in mice. FEMS Immunol Med Microbiol 56: 204-211, 2009.
10. Park EJ, Cheenpracha S, Chang LC, Kondratyuk TP and Pezzuto JM: Inhibition of lipopolysaccharide-induced cyclooxygenase-2 and inducible nitric oxide synthase expression by 4-[(2'-O-acetyl-α-L-rhamnosyloxy)benzyl]isothiocyanate from *Moringa oleifera*. Nutr Cancer 63: 971-982, 2011.
11. Kaltschmidt B and Kaltschmidt C: NF-kappaB in the nervous system. Cold Spring Harb Perspect Biol 1: a001271, 2009.
12. Mehan S, Meena H, Sharma D and Sankhla R: JNK: A stress-activated protein kinase therapeutic strategies and involvement in Alzheimer's and various neurodegenerative abnormalities. J Mol Neurosci 43: 376-390, 2011.
13. Corrêa SA and Eales KL: The role of p38 MAPK and its substrates in neuronal plasticity and neurodegenerative disease. J Signal Transduct 2012: 649079, 2012.
14. Ha SK, Moon E, Ju MS, Kim DH, Ryu JH, Oh MS and Kim SY: 6-Shogaol, a ginger product, modulates neuroinflammation: A new approach to neuroprotection. Neuropharmacology 63: 211-223, 2012.
15. Park SY, Jin ML, Kim YH, Kim Y and Lee SJ: Anti-inflammatory effects of aromatic-turmerone through blocking of NF-κB, JNK, and p38 MAPK signaling pathways in amyloid β-stimulated microglia. Int Immunopharmacol 14: 13-20, 2012.

16. Song MY, Bae UJ, Lee BH, Kwon KB, Seo EA, Park SJ, Kim MS, Song HJ, Kwon KS, Park JW, *et al*: *Nardostachys jatamansi* extract protects against cytokine-induced beta-cell damage and streptozotocin-induced diabetes. World J Gastroenterol 16: 3249-3257, 2010.
17. Liu QF, Jeon Y, Sung YW, Lee JH, Jeong H, Kim YM, Yun HS, Chin YW, Jeon S, Cho KS, *et al*: *Nardostachys jatamansi* ethanol extract ameliorates Aβ42 cytotoxicity. Biol Pharm Bull 41: 470-477, 2018.
18. Aisa R, Yu Z, Zhang X, Maimaitiyiming D, Huang L, Hasim A, Jiang T and Duan M: The effects of aqueous extract from Nardostachys chinensis batalin on blood pressure and cardiac hypertrophy in two-kidney one-clip hypertensive rats. Evid Based Complement Alternat Med 2017: 4031950, 2017.
19. Chen YP, Ying SS, Zheng HH, Liu YT, Wang ZP, Zhang H, Deng X, Wu YJ, Gao XM, Li TX, *et al*: Novel serotonin transporter regulators: Natural aristolane- and nardosinane- types of sesquiterpenoids from Nardostachys chinensis Batal. Sci Rep 7: 15114, 2017.
20. Yoon CS, Kim KW, Lee SC, Kim YC and Oh H: Anti-neuroinflammatory effects of sesquiterpenoids isolated from *Nardostachys jatamansi*. Bioorg Med Chem Lett 28: 140-144, 2018.
21. Hwang JS, Lee SA, Hong SS, Han XH, Lee C, Lee D, Lee CK, Hong JT, Kim Y, Lee MK, *et al*: Inhibitory constituents of Nardostachys chinensis on nitric oxide production in RAW 264.7 macrophages. Bioorg Med Chem Lett 22: 706-708, 2012.
22. Rao X, Huang X, Zhou Z and Lin X: An improvement of the 2^(-delta delta CT) method for quantitative real-time polymerase chain reaction data analysis. Biostat Bioinforma Biomath 3: 71-85, 2013.
23. Yoon CS, Kim DC, Lee DS, Kim KS, Ko W, Sohn JH, Yim JH, Kim YC and Oh H: Anti-neuroinflammatory effect of aurantiamide acetate from the marine fungus *Aspergillus* sp. SF-5921: Inhibition of NF-κB and MAPK pathways in lipopolysaccharide-induced mouse BV2 microglial cells. Int Immunopharmacol 23: 568-574, 2014.
24. Kim DC, Lee HS, Ko W, Lee DS, Sohn JH, Yim JH, Kim YC and Oh H: Anti-inflammatory effect of methylpenicinoline from a marine isolate of *Penicillium* sp. (SF-5995): Inhibition of NF-κB and MAPK pathways in lipopolysaccharide-induced RAW264.7 macrophages and BV2 microglia. Molecules 19: 18073-18089, 2014.
25. An RB, Min BS, Na MK, Chang HW, Son KH, Kim HP, Lee HK, Bae K and Kang SS: Iridoid esters from *Patrinia saniculaefolia*. Chem Pharm Bull (Tokyo) 51: 583-585, 2003.
26. Zhang Y and Dong C: Regulatory mechanisms of mitogen-activated kinase signaling. Cell Mol Life Sci 64: 2771-2789, 2007.
27. Nguyen MD, Julien JP and Rivest S: Innate immunity: The missing link in neuroprotection and neurodegeneration? Nat Rev Neurosci 3: 216-227, 2002.
28. Lappas M, Permezel M, Georgiou HM and Rice GE: Nuclear factor kappa B regulation of proinflammatory cytokines in human gestational tissues in vitro. Biol Reprod 67: 668-673, 2002.
29. Agostinho P, Cunha RA and Oliveira C: Neuroinflammation, oxidative stress and the pathogenesis of Alzheimer's disease. Curr Pharm Des 16: 2766-2778, 2010.
30. Zhang G and Ghosh S: Toll-like receptor-mediated NF-kappaB activation: A phylogenetically conserved paradigm in innate immunity. J Clin Invest 107: 13-19, 2001.
31. Bennett AM and Tonks NK: Regulation of distinct stages of skeletal muscle differentiation by mitogen-activated protein kinases. Science 278: 1288-1291, 1997.